Arab J Sci Eng (2015) 40:1743–1756
DOI 10.1007/s13369-015-1649-2

RESEARCH ARTICLE - MECHANICAL ENGINEERING

Experimental and Theoretical Comparative Study of Performance and Emissions for a Fuel Injection SI Engine with Two Octane Blends

A. E. Khalifa[1,2] · M. A. Antar[1] · M. S. Farag[2]

Received: 1 November 2014 / Accepted: 26 March 2015 / Published online: 22 April 2015

Abstract Experimental and theoretical investigations are carried out to study and compare the effect of using two gasoline blends, namely octane 91 and octane 95, on the performance and exhaust emissions of a modern fuel injection SI engine at different engine speeds and loads. Theoretical combustion model is able to predict the engine performance when compared to the experimental findings. Results show that the engine performances of both fuels are comparable, with marginal differences, under the tested operating conditions, practically for engine speeds less than 3500 rpm. Higher power and less specific fuel consumption are observed when octane 91 fuel is used compared with octane 95 blend. Both blends do not show a tendency of knock occurrence. In general, both fuels show similar trends for CO, CO_2 and NO_x concentrations in the exhaust, whereas the unburned hydrocarbons are slightly higher when octane 91 fuel is used. In the higher speed range between 3500 and 5000 rpm, a noticeable decrease in CO_2 concentration, an increase in specific fuel consumption and CO concentration are observed.

Keywords Engine performance and emissions · Octane 91 and octane 95 gasolines · Experimental testing · Modeling of combustion cycle · Knock tendency

✉ M. A. Antar
antar@kfupm.edu.sa

[1] Mechanical Engineering Department, King Fahd University of Petroleum and Minerals, Dhahran 31261, Saudi Arabia

[2] Mechanical Power Engineering Department, Menoufia University, Shebeen El-Kom, Egypt

List of symbols

a, b, c	Constants
A/F	Air-to-fuel ratio
BDC	Bottom dead center
BOC	Beginning of combustion
BP	Brake power
BSFC	Brake specific fuel consumption
CR	Compression ratio
D	Bore
E	Energy
g	Gibbs free energy
h_t	Convective heat transfer coefficient
K_1, K_2, K_3	Constants
K_P	Equilibrium constant
L	Length
m	Mass
N	Engine rpm
n	Number of moles
P	Pressure (total/partial)
Q	Heat transfer rate
R	Crank radius
R_u	Universal gas constant
S_θ	Position of the piston depending on crank angle
T	Temperature
t	Time
TDC	Top dead center
$u_{i,j}$	Constants
U_{PIS}	Mean piston speed
V	Volume
W	Work
x_i	Mole fraction for each species in the gas mixture inside the cylinder

Subscripts

c	Clearance
con	Connecting rod
cy	Cylinder
g	Gas
o	Ambient
ref	Beginning of compression stroke
st	Stroke

Greek symbols

ε	Emissivity
ΔH_o	Enthalpy of formation
γ_r	Residual exhaust gas ratio = 0.04
η_v	Volumetric efficiency
λ	Equivalence ratio
θ	Crank angle
ρ	Mass density
σ	Stefan–Boltzman constant (5.67×10^{-11} kW/m^2 K^4)

1 Introduction

Internal combustion engines in either major type of operating mode, spark ignition or compression ignition, are expected to continue to dominate as the major power source for automotive propulsion for the short- to medium-term future. This means that gasoline and diesel fuels from conventional fossil hydrocarbon sources or their substitutes will continue to be in demand. The octane number is one of the most important parameters determining the fuel quality. It has a direct effect on the engine performance and exhaust emissions at different speed and load conditions [1–4]. The octane number of a gasoline is a measure of its resistance to detonation (knocking), an uncontrolled explosion of the combustible mixture inside the engine cylinder. When knock occurs in operating engines, it causes reduced efficiency, increased heat transfer and, if it is severe, engine damage [1]. Octane requirement to avoid knocking is related to the engine type and engine operating conditions. Research octane number (RON) and motor octane number (MON) are measures of fuel anti-knocking performance. American cars use an octane scale derived from the average of both RON and MON, while in Saudi Arabia, only the RON scale is used [5].

The effect of gasoline octane number on effective power and fuel economy was investigated [6]. The engine required was tested with 91-RON and 95-RON. Results showed that the average fuel consumption using 95-RON is higher than that of 91-RON. Moreover, it was seen in this study that using higher-octane rating gasoline than engine requirement did not augment effective power. Another study [7] clearly reported that octane number plays an important role on concentrations of the exhaust emissions. Two different octane gasoline fuels, with 91 and 93 octane numbers, were conducted in a four-cylinder and four-stroke SI engine. The results demonstrated that as the octane number was increased from 91 to 93; CO concentration was boosted by 5 % approximately.

The effect of using higher-octane gasoline than that of engine requirement on the performance and exhaust emissions was experimentally studied [8] with a carburetor test engine. The engine that required 91-RON gasoline was tested using 95-RON and 91-RON. Results show that using octane ratings higher than the requirement of an engine not only decreases engine performance but also increases the concentrations of exhaust emissions such that 91 gasoline caused 5.7 % CO and 3.4 % HC lower than 95 octane gasoline. Therefore, using the correct gasoline required by the engine is more advantageous than using a higher-octane gasoline under all operating conditions. Although it has been explained that using correct gasoline is the best for the engine, people still prefer to use higher-octane gasoline. The effects of using different blending ratio gasoline–ethanol blended fuels on the pollution emission and the engine performance of a spark ignition engine were investigated experimentally [9]. It was found that heating value of blended fuel decreases as the ethanol content increases. They also showed that as the ethanol contents increase, the octane number of the blended fuels increases. They showed from the test that there is slight increment in fuel consumption and output torque of the engine when ethanol–gasoline blended fuel is used. A comparison between two gasolines with octane 90 and 97 is presented [10]. It was shown that the fuel with excessively high octane number deteriorates the fuel consumption, especially at low or middle loads. High-octane number gasoline suppresses the rate of combustion and increases the combustion duration, resulting in the increase in fuel consumption and THC concentrations. Isin and Uzunsoy [11] developed a model to predict the exhaust emissions of a spark ignition engine based on experimental data that were used to train the model. Anetor et al. [12] carried out a computational study to investigate the formation of nitrogen oxides from a spark ignition engine at two temperatures 2600 and 1900 K that represent typical operating conditions for the engines.

Improving spark ignition engines is a fundamental target due to knocking phenomenon, which is still in an early stage of understanding. Several publications indicated that inhomogeneities of the gas mixture may lead to this undesired mode of combustion [13]. The fundamental idea of this approach is a gas mixture that exhibits spatial differences of ignition time as a consequence of inhomogeneity and permits flame propagation due to local and sequentially proceeding auto-ignition [14–21]. Pressure and acoustic measurements can provide evidence whether the engine knocks or not. No information is available yet as to where or why the engine

knocks. In addition, the effect of changing the octane number of the fuel on the knock intensity for the same engine has not been investigated significantly [22,23]. Previous investigations using a carburetor system mentioned that using higher octane number of gasoline on the engine results in a longer ignition delay and lower flame speed [24]. This can cause diminishing effective power [25]. However, at a given throttle position, engine power insignificantly changes with octane number [26]. In addition, the additives used to increase octane number also influence the emission concentrations. For instance, the tetra alkyl lead in gasoline is an important parameter influencing the contents of exhaust emissions [27]. The conventional carburetor spark ignition engines (SIEs) received significant attention in previous studies for the effect of the octane number on engine knocking and performance characteristics. However, new trends of SI engines are to use fuel injection and spray-guided direct fuel injection systems to meet the future requirements that include lower fuel consumption and reduced concentrations of pollutants.

Few years ago, a new octane 91 gasoline has been introduced in Saudi Arabia with 30 % lower prices compared with octane 95. However, it is widely believed that the higher octane rating makes the engine better in performance and emission concentrations. In this study, the engine performance and exhaust gas concentrations for both octane grades are compared under local operating conditions. Knocking tendency for both fuels is also compared. A modern spark ignition engine (SIE) with fuel injection system is used for testing as the majority of the cars in Saudi Arabia use similar system. The aim of this work is to provide a solid conclusion about using the two commercially available gasoline grades 91 and 95 in Saudi Arabia regarding performance and exhaust gas concentrations, with the same engine through experimental and theoretical investigations with evaluation of knock tendency. The outcome of this work will provide valuable information for local car users and recommendations to the local car dealers and engine manufacturers.

2 Modeling the Thermodynamic Cycle

In this section, modeling of the thermodynamic cycle inside the engine cylinder is presented to evaluate engine's performance parameters. The model is used to study the engine performance under different operating conditions and fuel types of different chemical compositions. The instantaneous pressure, temperature and cylinder volume as well as the concentration of different species are predicted. Other important parameters such as the mean effective pressure, power, *A*/*F* ratio and efficiency are calculated. The mixture of different species in the cylinder is considered homogeneous and at equilibrium. The gas mixture is treated as one-dimensional flow, compressible fluid and time depended. The heat losses

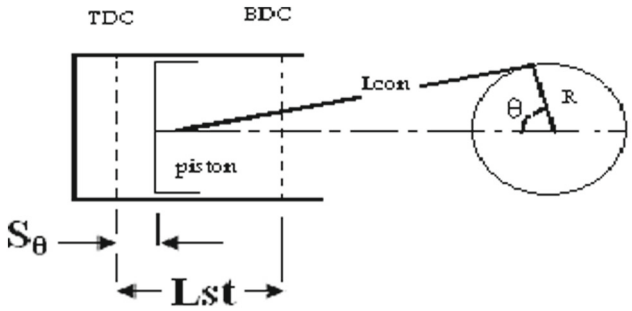

Fig. 1 Crank–slider mechanism

from the cylinder are taken into account. The dissociation of CO_2 is considered during the combustion and expansion processes. The conservation equations of mass and energy for the working mixture inside the cylinder are adopted with the kinematics of mechanical parts.

From the kinematics of the crank–slider mechanism shown in Fig. 1, the instantaneous piston displacement is calculated as follows:

$$S_\theta = [L_{\text{con}} + R] - \left[R \cdot \cos\theta + \sqrt{L_{\text{con}}^2 - (R \cdot \sin\theta)^2}\right] \quad (1)$$

The instantaneous cylinder volume is calculated as follows:

$$V = V_\theta + V_{\text{c}} \quad (2)$$

where

$$V_\theta = \frac{\pi}{4} D^2 \cdot S_\theta$$

and

$$V_c = \frac{V_{\text{st}}}{(\text{CR} - 1)} = \frac{\frac{\pi}{4} D^2 \cdot L_{\text{st}}}{(\text{CR} - 1)}, \quad \text{L}_{\text{st}} = 2\text{R}$$

While the working fluid inside the cylinder is considered as a perfect gas, equation of state can be written as follows,

$$PV = n\text{R}_\text{U}\text{T} \quad (3)$$

The time-dependent differential conservation equation of energy representing the compression, combustion and expansion process is written as:

$$\frac{\text{d}Q}{\text{d}t} - p\frac{\text{d}V}{\text{d}t} = \frac{\text{d}E}{\text{d}t} \quad (4)$$

In the absence of any gas leakage between piston and cylinder walls, the mass of the working fluid is considered constant during the compression, combustion and expansion process.

Therefore, during these processes the following equation is considered.

$$m_{\text{reactants}} = m_{\text{products}} \tag{5}$$

The single-zone model is employed. The equations of chemical reaction at equilibrium, fraction of fuel burnt/total fuel injected per cycle per cylinder and fuel burning rate are considered.

For nondissociation combustion of hydrocarbon fuel, general forms of the chemical reactions are written for complete combustion, with excess air and with insufficient air, respectively, as:

$$\begin{aligned}
&\mathrm{C}_n\mathrm{H}_m + \lambda X_{\text{th}}(O_2 + 3.76\mathrm{N}_2) \rightarrow a\mathrm{CO}_2 + b\mathrm{H}_2\mathrm{O} + d\mathrm{O}_2 \\
&\qquad\qquad + 3.76\lambda X N_2 \\
&C_n H_m + \lambda X_{\text{th}}(O_2 + 3.76\mathrm{N}_2) \rightarrow a_1\mathrm{CO}_2 + b_1\mathrm{H}_2\mathrm{O} \\
&\qquad\qquad + d_1\mathrm{O}_2 + 3.76\lambda X N_2 \\
&\mathrm{C}_n\mathrm{H}_m + \lambda X_{\text{th}}(O_2 + 3.76N_2) \rightarrow a_2 C\,O_2 + b_2\mathrm{H}_2\mathrm{O} \\
&\qquad\qquad + d_2\mathrm{CO} + 3.76\lambda X N_2
\end{aligned} \tag{6}$$

where n and m are the number of carbon and hydrogen atoms in fuel, respectively,

and

$$\lambda = \frac{(A/F)_{\text{actual}}}{(A/F)_{\text{stoichiometric}}}$$

If the fuel contains oxygen, then the number of oxygen atoms in the fuel is included in the above balance equations. During the combustion process, part of the fresh mixture is burned and converted into products in an exothermic reaction. The combustion proceeds until all the amount of the fresh charge is burned completely. Watson model [28] is employed to calculate the fuel burning rate while considering dissociation. It suggests combining a premixed burning function and a diffusion burning function with a phase proportionality factor. Combustion duration is an arbitrary period in which combustion must be completed. A value of 125 crank angle degrees is considered for combustion period in the current model. The actual point at which combustion ceases has little significance since the rate decays exponentially to almost zero before combustion truly stops.

Due to the high temperature and pressure inside the cylinder during the combustion and expansion processes, dissociation takes place. The dissociation of carbon dioxide to carbon monoxide and oxygen is considered. The rate of formation of carbon dioxide is equal to the rate of formation of carbon monoxide and oxygen. The stoichiometric reaction for this case under equilibrium condition is:

$$\mathrm{CO} + \frac{1}{2}\mathrm{O}_2 \Leftrightarrow \mathrm{CO}_2 \tag{7}$$

The concentrations of CO_2, CO and O_2 are obtained from the following equation:

$$K_{\mathrm{P}} = \frac{P_{\mathrm{CO}_2}}{P_{\mathrm{CO}}\sqrt{P_{\mathrm{O}_2}}} \tag{8}$$

where P_{CO_2}, P_{CO} and P_{O_2} are the partial pressures of CO_2, CO and O_2, respectively.

The equilibrium constant K_{P} is determined from Gibbs function [29] for the considered reactants as follows:

$$\ln K_{\mathrm{P}} = \sum\left(\frac{n_i \cdot g(T)}{R_U \cdot T}\right)_R - \sum\left(\frac{n_i \cdot g(T)}{R_U \cdot T}\right)_P - \frac{\Delta \mathrm{H}_O}{R_{\mathrm{U}} \cdot T} \tag{9}$$

and

$$\frac{g_i(T)}{R_U.T} = u_{i,1}\,(1 - \ln T) - \sum_{j=2}^{j=5}\frac{u_{i,j}}{j-1}.T^{j-1} - u_{i,6} \tag{10}$$

Heat loss from combustion gases through the cylinder wall to the coolant strongly influences the thermodynamics of the engine cycle. This heat loss is an important part of the energy balance, which influences gas temperature and pressure, piston work, engine performance, and concentrations of emitted gases.

Heat losses from the working fluid are mainly due to convection from the gases and radiation from flame front to the cylinder wall. The heat flux is then calculated from the following general equation.

$$q = \frac{Q_{\text{loss}}}{A} = h\left(T_{\mathrm{g}} - T_{\mathrm{w}}\right) + \varepsilon \cdot \sigma\left(T_{\mathrm{g}}^4 - T_{\mathrm{w}}^4\right) \tag{11}$$

where h is the convective heat transfer coefficient, ε is the emissivity, and σ is the Stefan–Boltzmann constant. Considering the cylinder wall uncovered by the piston as the heat transfer surface, the area of heat transfer is written as $A_{\mathrm{h.t}} = \pi.\mathrm{D}.(\mathrm{S}_\theta + \mathrm{L}_{\mathrm{c}})$, where S is the piston displacement from TDC and L_{c} is the clearance length.

Wand and Berry [30] stated that "Radiative heat transfer in IC engines can be divided into two parts: the nonluminous gas radiation and the luminous solid-particle (soot) radiation. In spark ignition (SI) engines, the radiation contributed by the soot particles can be neglected." In SI engines, Radiation from high temperature gases and the flame region to the combustion chamber wall is insignificant compared with convective heat transfer [1]. The correlation of the heat transfer coefficient was suggested by Woschni [31], which is considered the most commonly used semiempirical correlation based on experimental results.

$$q = \frac{Q_{\text{loss}}}{A} = h_{\text{t}}\left(T_{\text{g}} - T_{\text{w}}\right) \tag{12}$$

The convective heat transfer coefficient, h_{t}, requires an average wall temperature and uses the dimensionless analysis to obtain the coefficient of heat transfer as [30–32]:

$$h_{\text{t}} = \frac{K_1.P^{0.8}}{D^{0.2}.T^{0.53}}\left[K_2 \cdot U_{\text{pis}} + K_3.\frac{V \cdot T_{\text{ref}}}{P_{\text{ref}} \cdot T_{\text{ref}}}.(P - P_{\text{m}})\right]^{0.8} \tag{13}$$

$$\frac{P_{\text{m}}}{P_{\text{ref}}} = \left(\frac{V_{\text{ref}}}{V}\right)^{n}, n = 1.32 \tag{14}$$

$$U_{\text{pis}} = \frac{2 \cdot L_{\text{st}} \cdot N}{60} \quad \text{m/s} \tag{15}$$

where T_{ref}, P_{ref} and V_{ref} are temperature, pressure and volume at the beginning of the compression stroke. K_1, K_2 and K_3 are constants.

The possible effects of surface scales or deposits on either side of the cylinder wall are not considered, and the heat losses through leaks at the valve seats or at the gap between the liner and the piston are neglected.

The cylinder air capacity depends on the density of air at the end of intake stroke. The volumetric efficiency can be expressed mathematically as follows.

$$\eta_v = \frac{m_{\text{air, acual}}}{m_{\text{air, theor}}} \tag{16}$$

While the actual mass of air flow rate is a measured quantity, the theoretical mass of air flow rate can be calculated as follows:

$$m_{\text{air, theortically}} = \frac{\rho_{\text{air}} \cdot V_{\text{st}} \cdot Z \cdot N}{i \cdot 60} \quad \text{kg/s} \tag{17}$$

where Z is the number of cylinders, $\boldsymbol{i}$ is a constant which equals to 2, and air density $\rho_{\text{air}} = \dfrac{P_{\text{l}}}{R_{\text{air}} \cdot T_{\text{l}}}$

The compression stroke is considered to begin at BDC. The initial air temperature at the beginning of compression stroke is calculated as:

$$T_{\text{i}} = \frac{T_{\text{O}} + \Delta T_{\text{w}} + \gamma_{\text{r}} \cdot T_{\text{r}}}{1 + \gamma_{\text{r}}} \tag{18}$$

T_{O}: Ambient air temperature = 300°K.
γ_{r} : Residual exhaust gas ratio = 0.04.
ΔT_{w} : Temperature increase due to the heat transferred from cylinder wall.
T_{r} : Residual gas temperature.
The number of moles inside the cylinder is given by the equation of state as follows:

$$n_{\text{t}} = \frac{P_{\text{cy}} \cdot V_{\text{cy}}}{R_{\text{u}} \cdot T_{\text{cy}}} \tag{19}$$

The total number of moles is kept constant during the compression stroke at which no chemical reaction is considered. The instantaneous cylinder volume is calculated from previously mentioned crank slider mechanism. The temperature and pressure inside the cylinder are obtained from both the energy equation and the equation of state. These equations are solved numerically using a finite difference technique and applied to two consecutive finite points. The energy equation for closed system is written as:

$$E_2(T_2) - E_1(T_1) + \frac{P_1 + P_2}{2} \cdot (V_2 - V_1) - Q_{\text{loss}} = 0.0 \tag{20}$$

with

$$E_1(T_1) = n_{\text{t}} \cdot \sum_{i=1}^{k} X_i \cdot R_{\text{u}}\left(\left[\sum\nolimits_{J=1}^{5} a_i \cdot T_1^J\right] - T_1\right) + n_{\text{t}} \sum_{i=1}^{k} X_i \cdot E_O(0)$$

$$E_2(T_2) = n_{\text{t}} \cdot \sum_{i=1}^{z} X_i \cdot R_u\left(\left[\sum\nolimits_{J=1}^{5} a_i \cdot T_2^J\right] - T_2\right) + n_{\text{t}} \sum_{i=1}^{z} X_i \cdot E_O(0)$$

where: a_{i} : Polynomial coefficients for enthalpy of different species [33]
X_{i} : Mole fraction for each species in the gas mixture inside the cylinder.
E_{o} : Internal energy or enthalpy at zero absolute temperature.

3 Experimental Setup

The engine used is an Armfield self-contained integrated four- cylinder, 1.0-l, water-cooled and normally aspirated laboratory engine test bed, as shown in Fig. 2. It is connected to a variable load eddy current, air-cooled dynamometer which acts as a brake, allowing direct measurement of engine torque. The engine is based on a 1-l four-cylinder automotive engine used in Volkswagen Polo car with 67.1 mm bore diameter and 70.6 mm stroke. The engine nominal power is 37 kW at 5000 rpm, and nominal torque is 86 Nm at 3400 rpm. The engine frame houses fuel tanks, battery, electrical enclosures and other accessories. The system is equipped with sensors for engine speed, torque, air flow, cooling water temperature (inlet and outlet of heat exchanger), cooling water flow and exhaust gas lambda sensor. The eddy current dynamometer provides a variable load on the engine, allowing the characteristic power and torque curves to be produced in the

Fig. 2 Photograph of engine and dynamometer test bed

laboratory. The whole system is designed to be linked to a personal computer equipped with special software such that throttle and brake load are controlled by the computer. This provides real-time monitoring of the various sensors, with a wide range of data logging and graphical display options. Each experiment was repeated at least three times to ensure repeatability of the results. The uncertainties in the reported performance parameters are estimated to be 5 %.

4 Results and Discussion

Table 1 shows the composition and properties of octane 91 and octane 95 gasoline fuels tested in the engine. The composition of the gasoline 91 and 95 was determined using a gas chromatographic PONA analyzer. These values are used also as input for the mathematical model.

Table 1 Composition and properties of octane 91 and 95 gasoline blends

	Octane 91	Octane 95	Unit
Carbon	83.98	84.11	wt%
Hydrogen	13.65	13.19	wt%
Oxygen	2.37	2.70	wt%
Density (15°C)	0.7277	0.7406	g/cm3
Vapor pressure (37.78°C)	62.0	68.5	kPa
Average molecular weight	88.00	89.45	
Heating value	43932	43304	kJ/kg
CHO composition	$C_{6.2}H_{12.0}O_{0.1}$	$C_{6.2}H_{11.6}O_{0.1}$	

4.1 Results of Mathematical Model

The following figures show and compare the model results for octane 91 and octane 95 gasoline blends in terms of performance parameters, namely brake power, specific fuel consumption and *A*/*F* ratio. Figure 3 shows that octane 91 fuel results in slightly higher power compared with octane 95 fuel. This is linked to the higher heating value of 91 as shown in Table 1. It is worth to mention that this result is also verified experimentally as shown in the next section of detailed experimental results. Figure 4 shows the comparison of model results at the some throttle openings (25, 50, 75 % and WOT) and speed range for specific fuel consumption. It shows that there are insignificant differences between octane 91 and octane 95 gasoline. Moreover, as the throttle opening increases, the differences in sfc between the two fuel blends diminish.

4.2 Validation of the Mathematical Model

In order to validate the mathematical model, a set of runs was carried out at conditions similar to the experimental ones. The experimental values for equivalence ratio, the volumetric efficiency and the exhaust gas temperature are used as input to the model for each corresponding engine speed and throttle opening. The output brake power (BP), the specific fuel consumption (BSFC) and air-to-fuel ratio (A/F) are presented for comparison and validation. For demonstration, some selected cases are presented in Fig. 5 that shows the comparisons between the model predictions against the experimentally measured values for gasoline 95 at 50 and 100 % throttle openings, under a variable speed test. In general, the mathematical model shows very close results to experimental findings as shown in the figure. The model

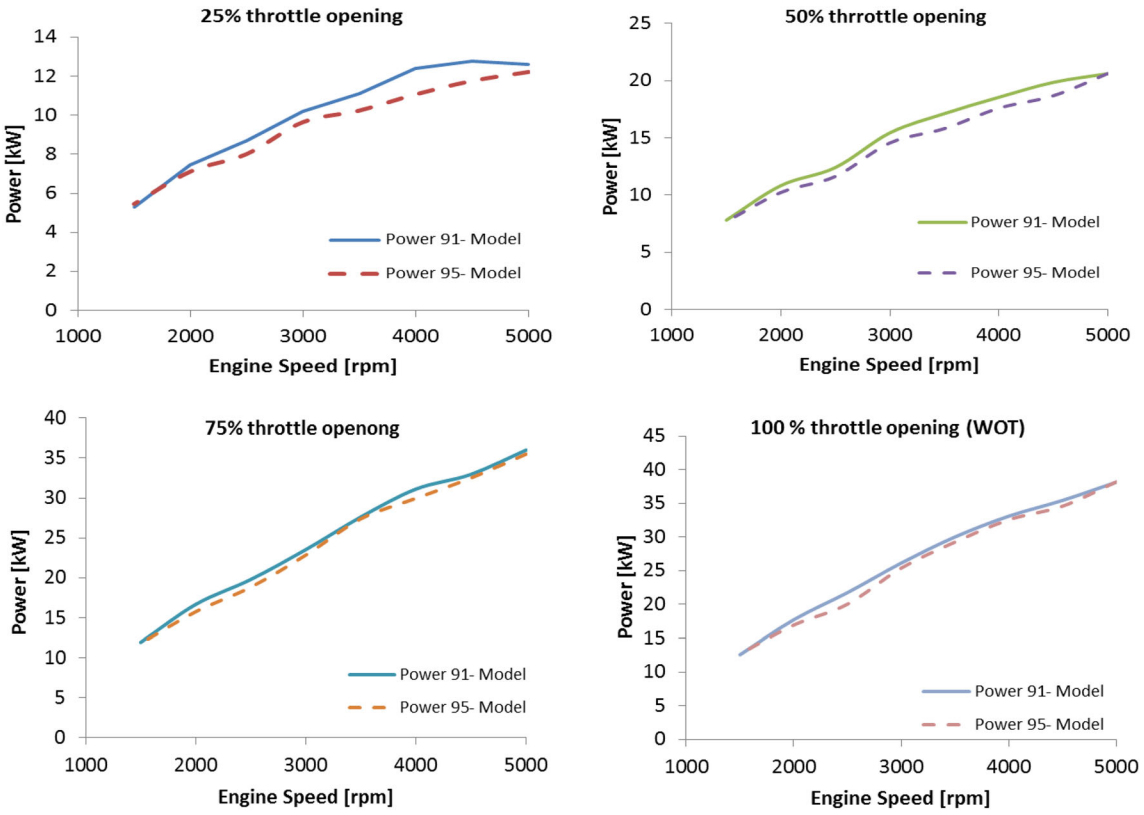

Fig. 3 Comparison between both fuels for power output model results

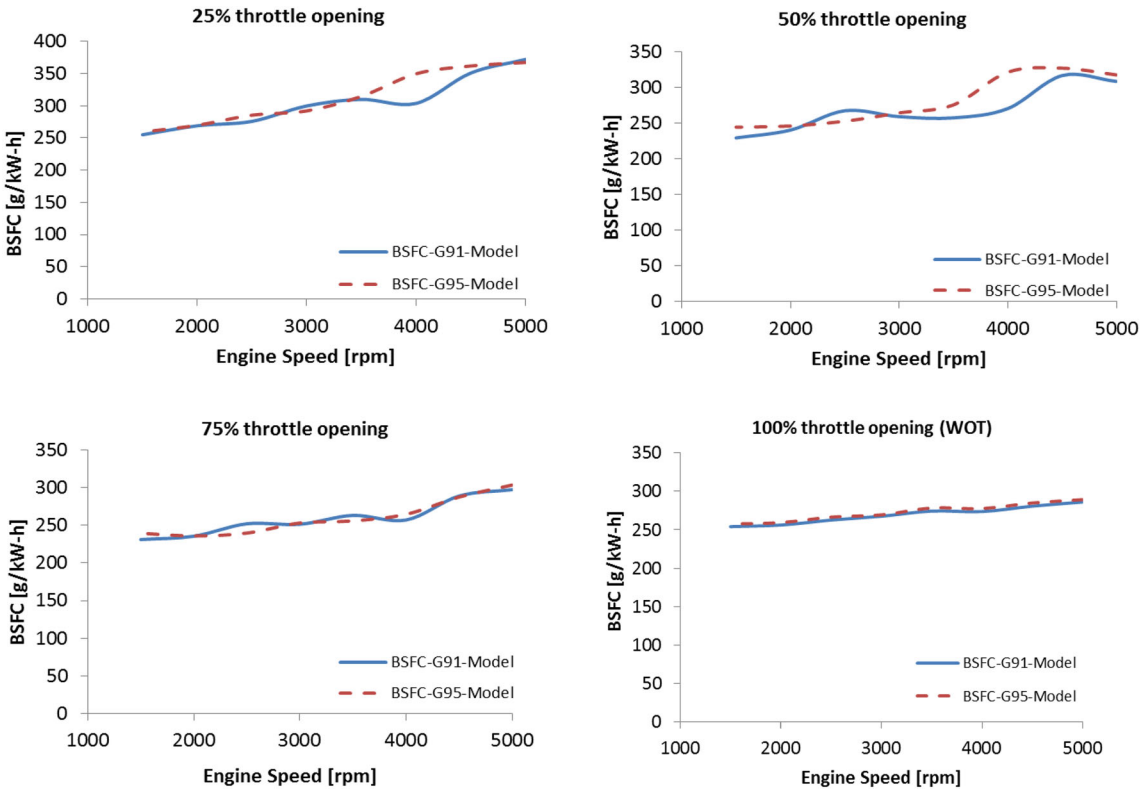

Fig. 4 Comparison between both fuels for specific fuel consumption model results

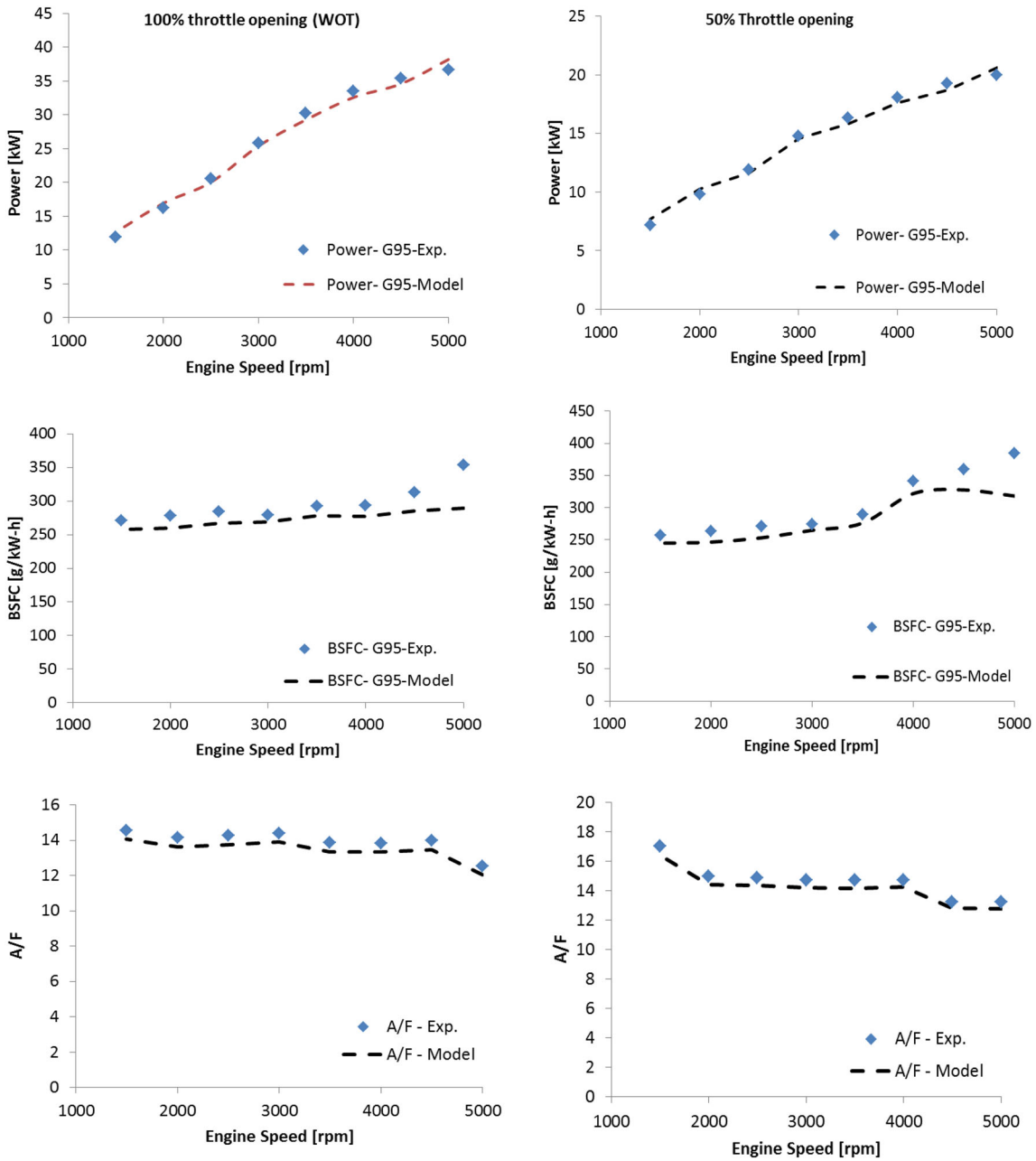

Fig. 5 Comparisons between experimental and model results for gasoline octane 95

prediction for the output power is considered excellent for the tested range of engine speeds. Similar trend was found for the calculated and measured air-to-fuel ratio. The model results for SFC showed good agreement with experimental values except for speeds 4000 rpm where noticeable differences between calculated and measured values are clear. In general, the mathematical model is able to predict the engine performance very well and can be used to perform a comprehensive study on the engine variables.

4.3 Detailed Experimental Results

Before running the experiments, enough amounts of commercial gasolines octane 91 and octane 95 were secured from a normal road fuel station to avoid discrepancies in fuel properties that may differ from batch to batch. Engine performance and concentrations of exhaust gases are measured at different engine speeds and loads for comparisons. The investigation range for engine speed is from 1500 to 5000

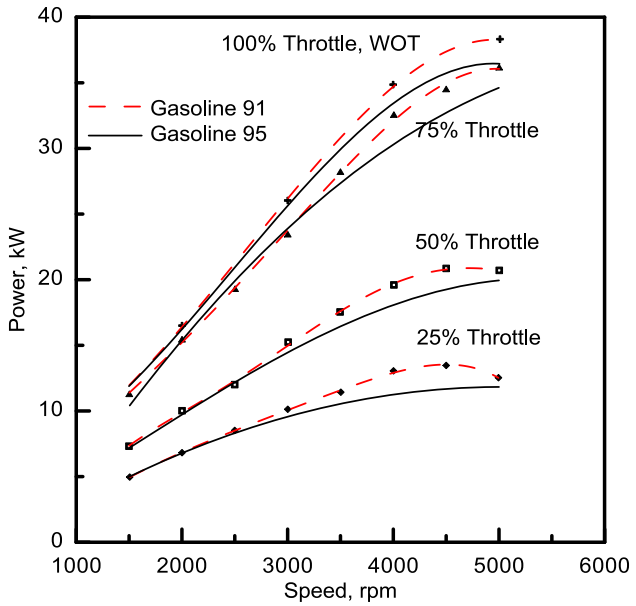

Fig. 6 Comparison between octane 95 and octane 91 fuels—power output

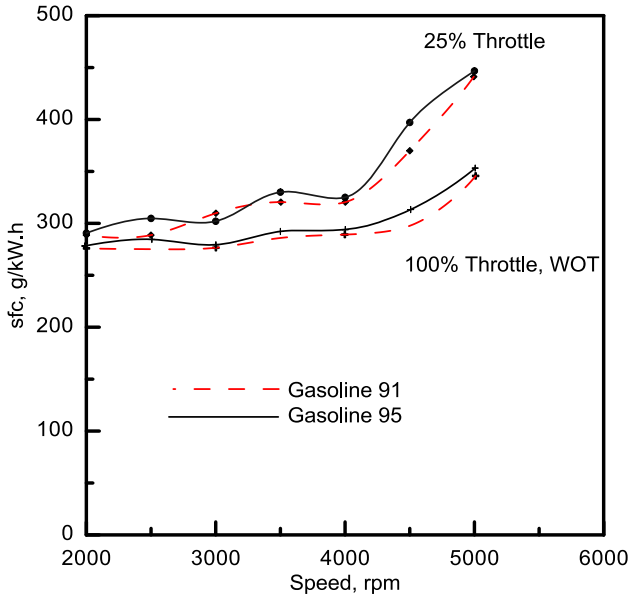

Fig. 7 Comparison between octane 95 and octane 91 fuels—bsfc

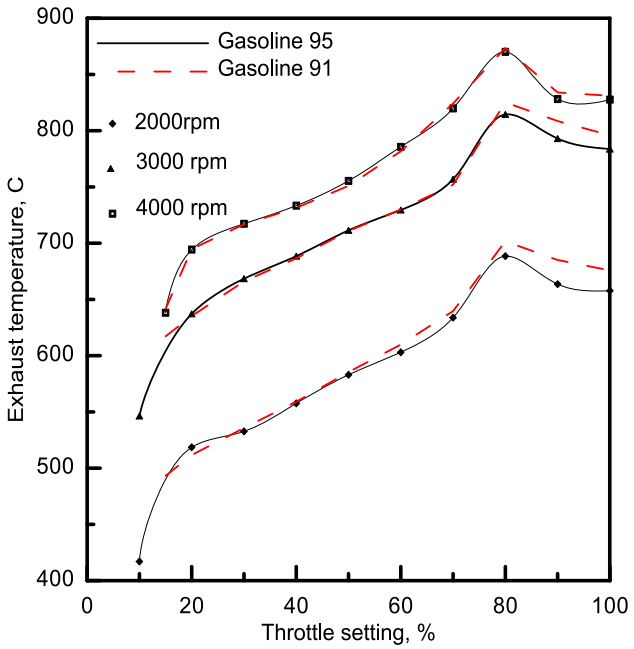

Fig. 8 Comparison between octane 95 and octane 91 fuels—exhaust gas temperature

rpm. The lowest stable speed for the engine was found to be 1500 rpm. The tested throttle openings are 25, 50, 75 and 100 % (wide open throttle, WOT). Cooling water flow rate is kept constant for all tests. The engine control unit automatically adjusts the air-to-fuel ratio. Fuel consumption is calculated from the injection system and the injection mode. Air flow rate into the engine is measured using an orifice meter and a differential pressure transducer at the air suction pipe.

Figure 6 shows the measured brake power at variable speeds for different throttle openings. It shows that using octane 91 fuel results in slightly higher power than using octane 95, especially for speeds higher than 3000 rpm. The differences are more consistent at higher throttle openings that correspond to higher load conditions. The increase in power with octane 91 fuel can be attributed to the higher hydrogen content in the fuel and its slightly higher heating value as shown in Table 1. Power normally increases with engine speed and throttle opening to fulfill the needs of engine loads.

The comparison in terms of brake specific fuel consumption (bsfc) is depicted in Fig. 7 for selected throttle openings. The figure shows insignificant variation in bsfc between both fuels with engine speed for the tested throttle settings. It may be noticed that slightly less fuel consumption for the engine operating with octane 91 compared with octane 95 is due to the slightly higher power of octane 91 fuel compared with octane 95 as shown in Fig. 6. It is noticed that bsfc is less at higher throttle openings indicating that engine economical range of operation is close to WOT. Part loads increase the sfc value compared with wide open throttle where optimum fuel quantity versus load is achieved [34]. Changing the fuel type has an insignificant effect on the exhaust gas temperature as shown in Fig. 8 for both fuels at different speeds and loads. This insignificant variation indicates that the temperature inside the cylinder during combustion cycle is relatively the same for both fuels. Consequently, the maximum temperature inside the cylinder is not affected significantly by changing the fuel octane number from 91 to 95.

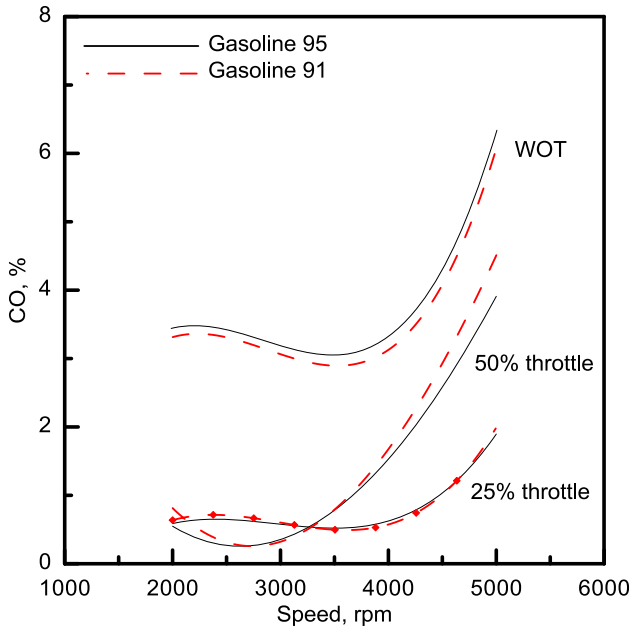

Fig. 9 Variation in exhaust CO concentrations with engine speed at different loads for both fuels

Consequently, the NOx concentrations are expected to be comparable when burning both fuels inside the engine.

4.4 Exhaust Emissions

Exhaust gas concentrations are measured during variable speed tests at different throttle openings. A gas analyzer (Applus+ AutoLogic exhaust gas analyzer, 5 gas version) is used to analyze engine exhaust at different operating conditions. The device measures HC, CO, CO_2, O_2, NO_x and air-to-fuel ratio. The probe is inserted in the engine exhaust tail pipe at a specified location for all tests. The engine operating conditions are set, and after becoming stable, samples are continuously recorded over a time period of at least one minute. Figure 9 shows a comparison of CO concentrations in the exhaust for both fuels. There are insignificant differences between CO concentrations for both fuels at different speeds and loads. Generally speaking, increasing the engine speed increases the CO concentrations for both fuels because higher speeds correspond to shorter time allocated for the combustion process leading to incomplete combustion. Higher loads would also require more fuel to be burned and accordingly result in higher CO concentrations in the exhaust.

Variations in exhaust CO_2 concentrations with variable speed tests and different loads are shown in Fig. 10. Gasoline 91 produces more CO_2 concentrations at 25 and 50 % throttle. Increasing the throttle opening while operating at moderate speeds results in similar exhaust CO_2 concentrations for both fuels. Increasing speed from 2000 to 4000 rpm has no effect on CO_2 concentrations for all loads. Above 4000 rpm, the exhaust CO_2 concentrations rapidly decrease for all loads that would be due to shorter time for complete combustion that produces more CO and would not have enough time for oxidizing CO to CO_2. This result can also be linked to the increased amount of fuel injected to the engine combustion chamber to cope with the increased engine load. It is interesting to note that the percentage of CO witnessed an increase in load from 25 % to WOT and CO_2 experiences an opposing trend, so that as the load increases, CO_2 decreases due to less conversion of CO to CO_2.

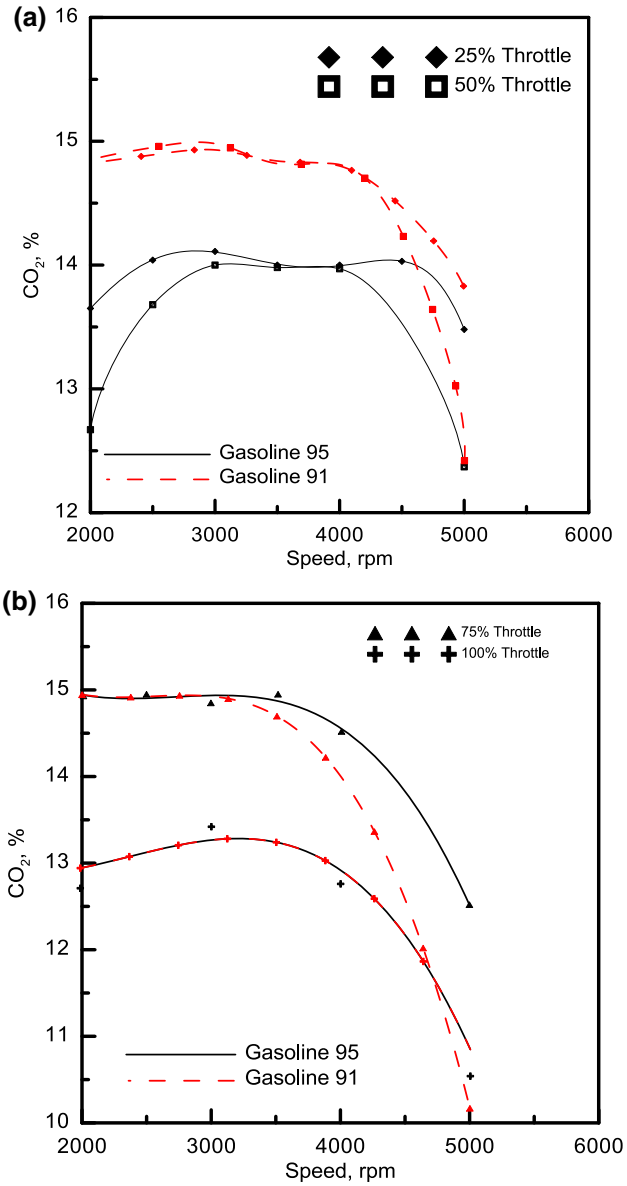

Fig. 10 Variation in exhaust CO_2 concentrations with engine speed at different loads for both fuels

A similar behavior was observed for HC concentrations in the exhaust gases as shown in Fig. 11.There are insignificant differences between exhaust HC concentrations for both

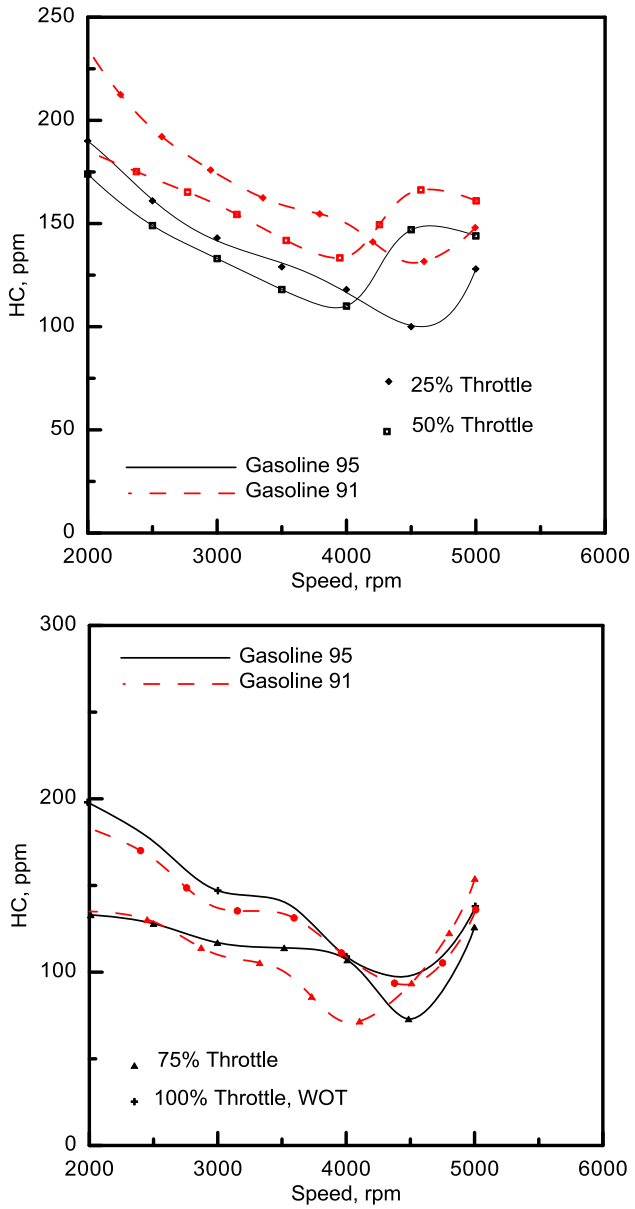

Fig. 11 Variation in exhaust HC concentrations with engine speed at different loads for both fuels

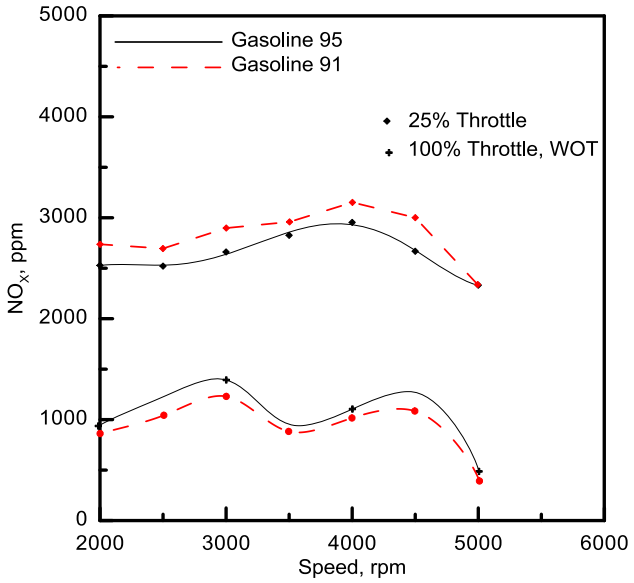

Fig. 12 Variation in exhaust NO_x concentrations with engine speed at different loads for both fuels

fuels at different speeds, practically above 50 % throttle. An increase in HC corresponding to octane 91 fuel does exist at lower loads (25 and 50 %) that can be attributed to the slightly higher hydrogen content in the 91 octane fuel as indicated in Table 1. A decrease in hydrocarbon emissions is monitored as the speed increases due to better mixing of fuel and air in the combustion chamber. Figure 12 shows samples of the variation in exhaust NO_x concentrations for variable speed test at different throttle settings. The figure shows that running the engine at WOT results in low NO_x emissions. In general, both fuels are producing similar rates of NO_x concentrations under the same engine operating conditions. This is expected since the temperature of the exhaust is the same for both fuels as shown in Fig. 8. However, it can be noticed that octane 91 fuel produces slightly more NO_x at low throttle settings and octane 95 produces slightly higher NO_x at high throttle settings.

5 Knock Tendency

Knock is one of the ways used to indicate the combustion abnormalities. "Knock is defined as the noise transmitted through the engine when spontaneous ignition of fuel gas mixture or residual gases are located at the end of the combustion chamber ahead of the propagating flame" [1]. It results in a sudden release of chemical energy that increases local pressure tremendously and leads to propagation of the pressure waves across the combustion chamber. Although it is more severe in WOT conditions, characteristics can be monitored at lower loads. Pressure variation during combustion cycle can be used to identify the knock tendency. High fluctuations or spikes in pressure reading (or graph) are an indication of knock in the engine.

Both fuels used in this study, octane 91 and octane 95, are high-rated fuels. They already have anti-knock additives since they are both commercially used. Burning both fuels under similar operating conditions for the same engine provides a good comparison for their tendency to knock. One of the engine's four cylinders is equipped with a piezoelectric pressure sensor (Kistler, spark plug Type 6117B, integrated with miniaturized piezoelectric high temperature,

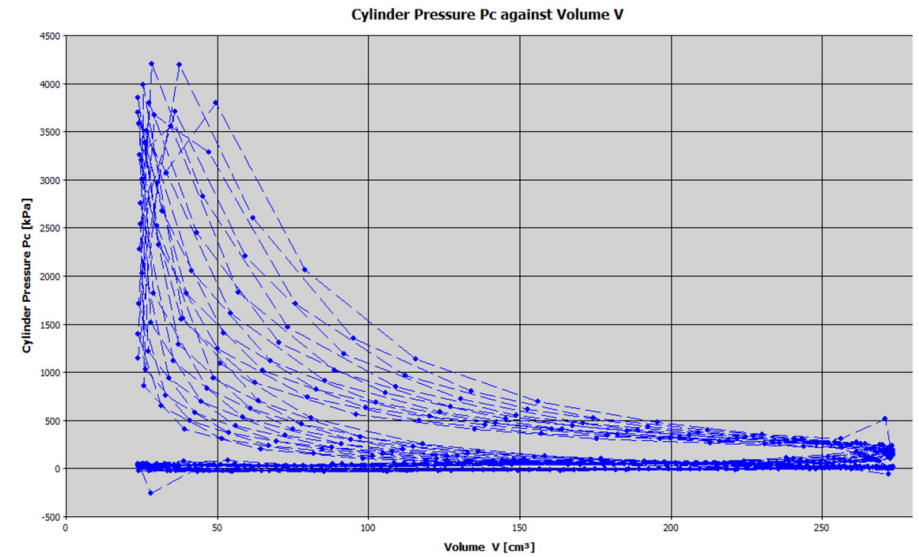

(a) Gasoline octane 91

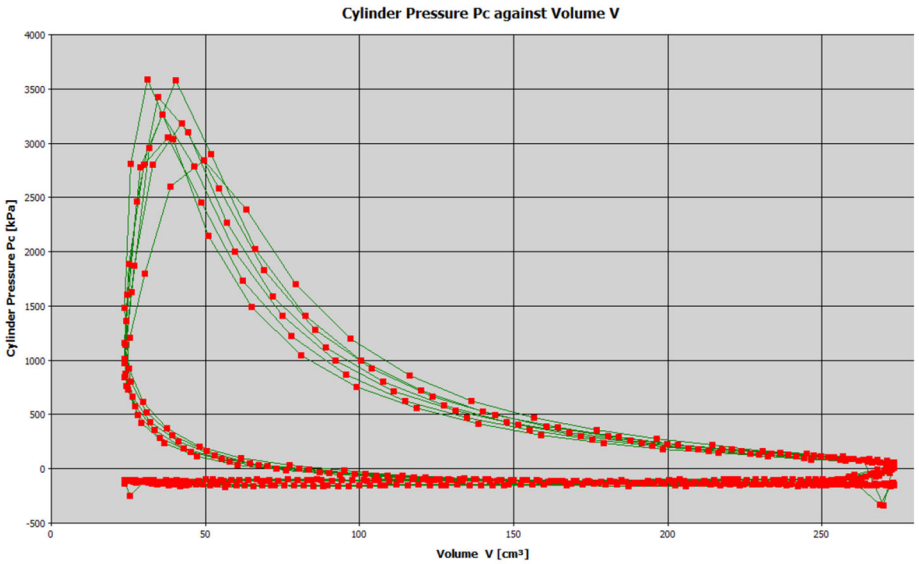

(b) Gasoline octane 95

Fig. 13 P–V diagrams for gasoline octane 91 and 95 at 50 % throttling and 2000 rpm

cylinder pressure sensor with frequency up to 100 kHz) to measure pressure variation in crank angle over several combustion cycles. The output signal was transmitted from the pressure transducer to the data acquisition system, and the results were recorded. A sample of this data is shown in Fig. 13 at 50 % throttling and 2000 rpm for demonstration to show the P–V diagram for a number of consecutive cycles. More cycle to cycle variations are clearly shown in Fig. 13a for octane 91 fuel, whereas the pressure readings are more consistent in Fig. 13b for octane 95 fuel. This difference in pressure variation is a typical variation from cycle to cycle (and from cylinder to cylinder as well). The variation may be interpreted for smoother combustion of octane 95 but it does not indicate knock occurrences since abnormal spikes of pressure during the combustion cycle are absent.

6 Conclusions

Experimental and theoretical studies are performed to investigate the effect of using the two commercially available gasoline types octane 91 and 95, used in the local market of Saudi Arabia with a modern fuel injection spark ignition engine. Although the theoretical model is relatively simple, comparison between the model results and experiment findings for the engine performance showed a very good agreement. The effects of changing major independent para-

meters, namely engine speed and engine load, on the engine performance and exhaust gas concentrations were measured. In general, results showed similar performance trends for both fuels under different operating conditions. The difference of 4 points in octane number between the two fuels did not show a significant change in the performance or pollutant concentrations in the exhaust gases. However, using octane 91 gasoline resulted in slight improvement in terms of power output and lower specific fuel consumption compared with octane 95 gasoline. This can be attributed to higher heating value of octane 91 fuel. Insignificantly higher CO_2 and HC concentrations were observed when using octane 91 fuel in contrast to octane 95 at moderate speeds and loads. Both fuels showed similar trends for exhaust CO and NO_x concentrations. Experiments showed that cycle to cycle pressure variations were more pronounced for 91 octane fuel. However, it is important to state that using either octane 91 or octane 95 fuels did not show a tendency of knock occurrence in the measured cycle P–V diagram. Therefore, smoother drivability may be expected when octane 95 is used. Results of this study are believed to be useful for local car users, dealers and manufacturers to know that similar performance characteristics are expected when either fuel grade is used.

Acknowledgments The investigators acknowledge the support provided by KFUPM to carry out this research under the DSR project # IN090013.

References

1. Heywood, J.B.: Internal Combustion Engine Fundamentals. McGraw-Hill Book, Inc., New York (1988)
2. Batmaz, I.; Balc, M.; Salman, S.; Erdiller, B.: Experimental analysis of fuel economy and exhaust emissions at petrol engine vehicles. In: First Automotive Technology Congress with International Participation, Adana, Turkey, pp. 95–103 (1997)
3. Twu, C.; Coon, J.: A Generalized Interaction Method for the Prediction of Octane Numbers for Gasoline Blends. pp. 1–18. Simulation Science Inc., New York (1998)
4. Mogi, K.; Katsushi, H.; Arisawa, K.; Kobayashi, H.: Analysis and avoidance of pre-ignition in spark-ignition engines. JSAE Rev. **19**, 9–14 (1998)
5. Saudi Aramco, Private Communications (2008)
6. Sudsanguan, P.; Chanchaowna, S.: Using higher octane rating gasoline than engine requirement: loss or gain, Research Report of King Mongkuts University of Technology, Thailand (1999)
7. Sayin, C.; Kilicaslan, I.: Influence of octane number on exhaust emission in a spark-ignition engines. In: The First International Exergy, Energy and Environment Symposium, Izmir/Turkey, pp. 184–189 (2003)
8. Sayin, C.; Kilicaslan, I.; Canakci, M.; Ozsezen, N.: An experimental study of the effect of octane number higher than engine requirement on the engine performance and emissions. Appl. Therm. Eng. **25**, 1315–1324 (2005)
9. Hsieh, W.-D.; Chen, R.-H.; Wu, T.-L.; Lin, T.-H.: Engine performance and pollutant emission of an SI engine using ethanol–gasoline blended fuels. Atmos. Environ. **36**(3), 403–410 (2002)
10. Shen, Y.-T.; Wang, J.-Z.; Shuai, S.-J.; Wang, J.-X.: Effects of octane number on gasoline engine performance. Chin. Intern. Combust Engine Eng. **29**(5), 52–56 (2008)
11. Isin, O.; Uzunsoy, E.: Predicting the exhaust emissions of a spark ignition engine using adaptive neuro-fuzzy inference system. AJSE **38**, 3485–3493 (2013)
12. Anetor, L.; Odetunde, C.; Osakue, E.E.: Computational analysis of the extended Zeldovich mechanism. AJSE **39**(11), 8287–8305 (2014)
13. Pöschl, M.; Sattelmayer, T.: Influence of temperature inhomogeneities on knocking combustion. Combust. Flame **153**, 562–573 (2008)
14. Checkel, M.D.; Dale, J.D.: Pressure trace knock measurements in a current SI production engine, SAE No. 890243 (1989)
15. Brunt, M.F.; Pond, C.R.; Biundo, J.: Gasoline engine knock analysis using cylinder pressure data, SAE No. 980896 (1998)
16. Lee, J.H.; Hwang, S.H.; Lim, J.S.; Jeon, D.C.; Cho, Y.S.: A new knock detection method using cylinder pressure, block vibration and sound pressure signals from SI engine. SAE No. 981436 (1998)
17. Konig, G.; Sheppard, C.G.W.: End gas autoignition and knock in a spark ignition engine, SAE No. 902135 (1990)
18. Li, H.L.; Karim, G.A.: Modelling the performance of a turbo-charged spark ignition natural gas engine with cooled exhaust gas recirculation. J. Eng. Gas Turbine Power Trans. ASME **130**, 032804 (2008)
19. Apicella, B.; Di Palma, T.M.; Wang, X.; Velotta, R.; Armenante, M.; Spinelli, N.: A mass spectrometric study of gasoline anti-knocking additives-part 1: election impact ionization and fragmentation processes of MTBE. Int. J. Mass Spectrom. **262**, 105–113 (2007)
20. Mehl, M.; Faravelli, T.; Giavazzi, F.; Ranzi, E.; Scorletti, P.; Tardani, A.; Terna, D.: Detailed chemistry promotes understanding of octane number and gasoline sensitivity. Energy Fuels **20**, 2391–2398 (2006)
21. Liberman, M.A.; Ivanov, M.F.; Valiev, D.M.; Eriksson, L.E.: Hot spot formation by the propagating flame and influence of EGR on knock occurrence in SI engines. Combust. Sci. Technol. **178**, 1613–1647 (2006)
22. Schießl, R.; Dreizler, A.; Maas, U.: Comparison of different ways for image post-processing: detection of flame fronts. SAE No. 1999-01-3651 (1999)
23. Graf, N.; Gronki, J.; Schulz, C.; et al.: In-cylinder combustion visualization in an autoigniting gasoline engine using fuel tracer and formaldehyde-LIF imaging. SAE No. 2001-01-1924 (2001)
24. Sayen, C.: An Experimental investigation of the influence of higher octane number then engine requirement in engine performance and emissions. Technoloji **7**(3), 479–487 (2004)
25. Nagai, S.; Seko, T.: Trends of motor fuel quality in Japan. JSAE Rev. 457–462 (2000)
26. Chanchaowna, S.: The effect of gasoline octane number on engine performance. In: Research Report of King Mongkut's University of Technology. Thailand pp. 1–8 (1999)
27. Sayin, C.; Kilicaslan, I.: the effect of lead ratio on exhaust emission in a gasoline engine. J. Naval Sci. Eng. **1**(1), 111–119 (2003)
28. Watson, N.; Janota, M.S.: Turbocharging the Internal Combustion Engine. McMillan Publisher, London (1984)
29. Benson, R.; Whitehouse, N.D.: Internal Combustion Engines. Pergamon Press, Oxford (1979)
30. Wang C.S.; Berry, G.F.: Heat Transfer in Internal Combustion Engines, ASME Winter Annual Meeting, November 17–21, (1985)
31. Woschni, G.: Universally applicable equation for instantaneous heat transfer coefficient in the internal combustion engine, SAE paper 670931. SAE Trans. **76** (1967)
32. Yusaf, T.F.; Hoe, Sye; Fong, M.Z. Yusoff; Hussein, I.: Modeling of Transient Heat Flux in Spark Ignition Engine During Combustion

and Comparisons with Experiment. Am. J. Appl. Sci. **2**(10), 1438–1444 (2005)
33. Draper, C.S.: Pressure waves accompanying detonation in internal combustion engine. J. Aeronaut. Sci. **5** (1938)
34. Obert, E.: Internal Combustion Engines and Air Pollution, 3rd edn. Harper & Row Publishers, New York (1968)